Therapeutic activity of an interleukin-4/interleukin-13 dual antagonist on oxazolone-induced colitis in mice

Marion T. Kasaian,[1] Karen M. Page,[2] Susan Fish,[1] Agnes Brennan,[1] Timothy A. Cook,[1] Karen Moreira,[1] Melvin Zhang,[1] Michael Jesson,[3] Kimberly Marquette,[4] Rita Agostinelli,[4] Julie Lee,[2] Cara M. M. Williams,[5] Lioudmila Tchistiakova[4] and Paresh Thakker[6]

[1]*Immunoscience, Pfizer, Cambridge, MA,* [2]*BioTherapeutics Clinical Research, Pfizer, Cambridge, MA,* [3]*Drug Safety Research and Development, Pfizer, Cambridge, MA,* [4]*Global BioTherapeutic Technologies, Pfizer, Cambridge, MA,* [5]*Inflammation and Remodeling, Pfizer, Cambridge, MA, and* [6]*Boehringer Ingelheim Pharmaceuticals, Inc, Ridgefield, CT, USA*

Correspondence: Marion T. Kasaian, Department of Immunoscience, Pfizer Research, 610 Main Street, Cambridge, MA 02139, USA.
Email: marion.kasaian@pfizer.com
Senior author: Marion T. Kasaian

Summary

Interleukin-4 (IL-4) and IL-13 are critical drivers of immune activation and inflammation in ulcerative colitis, asthma and other diseases. Because these cytokines may have redundant function, dual targeting holds promise for achieving greater efficacy. We have recently described a bifunctional therapeutic targeting IL-4 and IL-13 developed on a novel protein scaffold, generated by combining specific binding domains in an optimal configuration using appropriate linker regions. In the current study, the bifunctional IL-4/IL-13 antagonist was evaluated in the murine oxazolone-induced colitis model, which produces disease with features of ulcerative colitis. The bifunctional IL-4/IL-13 antagonist reduced body weight loss throughout the 7-day course of the model, and ameliorated the increased colon weight and decreased colon length that accompany disease. Colon tissue gene expression was modulated in accordance with the treatment effect. Concentrations of serum amyloid P were elevated in proportion to disease severity, making it an effective biomarker. Serum concentrations of the bifunctional IL-4/IL-13 antagonist were inversely proportional to disease severity, colon tissue expression of pro-inflammatory genes, and serum amyloid P concentration. Taken together, these results define a panel of biomarkers signifying engagement of the IL-4/IL-13 pathway, confirm the T helper type 2 nature of disease in this model, and demonstrate the effectiveness of dual cytokine blockade.

Keywords: bifunctional; colitis; cytokine.

Introduction

Interleukin-4 (IL-4) and IL-13 are key immunoregulatory cytokines, whose dysregulation may contribute to a range of inflammatory disease states, including ulcerative colitis (UC) and asthma. Although they are both T helper type 2 (Th2) cytokines, IL-4 and IL-13 can have distinct functional roles. IL-4 is a critical Th2-skewing cytokine and acts to direct immune responses, whereas IL-13 functions primarily as an effector cytokine, driving epithelial and fibrotic responses.[1] A bifunctional molecule targeting murine IL-4 and IL-13 on a novel multi-specific protein platform[a] was developed to neutralize both cytokines, with the goal of delivering a more potent therapeutic than could be achieved by blocking either cytokine alone. This may result from blocking the distinct actions of the separate agents, or from blocking the combined effect of their cooperative interactions and functional overlap.

Abbreviations: DAI, disease activity index; IBD, inflammatory bowel disease; IL-4, interleukin-4; mAb, monoclonal antibody; SAP, serum amyloid P; STAT6, signal transducer and activator of transcription 6; Th2, T helper type 2; UC, ulcerative colitis; V_H, V_L, heavy-chain and light-chain variable regions

In UC, IL-4 and IL-13 cytokine transcripts are detectable at lesion sites of active disease, both in the tissue and in infiltrating mononuclear cells.[2–5] Both IL-4 and IL-13 can drive pathogenic mechanisms, including impaired resistance in human intestinal epithelial monolayers, that may contribute to disease.[4,6] In accordance with this, reduced IL-13 secretion from infiltrating lamina propria mononuclear cells has been associated with disease amelioration following interferon-β treatment in subjects with UC.[7] The oxazolone-induced colitis model in mice recapitulates many of the disease features of human UC, including epithelial cell loss, depletion of goblet cells, inflammatory cell infiltration, oedema formation, haemorrhage and vascular dilatation.[8] In this model, mice lacking IL-13 are protected,[9] and IL-4 or IL-13 neutralization ameliorates disease.[3,10]

Interleukin-4 and IL-13 act through a shared receptor comprising IL-4Rα and IL-13Rα1 chains.[11] In addition, IL-4 activates T cells through the IL-4Rα/γ common receptor, which does not respond to IL-13.[11] Expression of both IL-4Rα and IL-13Rα1 chains is elevated in mucosal epithelial cells of UC lesions.[12] Expression of the IL-13 decoy receptor, IL-13Rα2, inducible in response to IL-4, IL-13 and tumour necrosis factor-α, is also elevated at sites of UC lesions,[12,13] indicative of cytokine activity. The IL-4 and IL-13 signalling responses are mediated by phosphorylation of the transcription factor, signal transducer and activator of transcription 6 (STAT6). The detection of pSTAT6 at sites of UC lesions, with intensity related to disease activity,[14] further supports involvement of IL-13 and/or IL-4 in disease pathogenesis.

The bifunctional IL-4/IL-13 antagonist consists of an N-terminal IL-13-binding domain derived from the murine IL-13Rα2 extracellular sequence, linked to the C57BL/6 IgG2c Fc, and connected by a linker sequence to a C-terminal IL-4-binding domain derived from anti-mouse IL-4 monoclonal antibody (mAb) 11B11.[15] The antagonist effectively binds to and inhibits the biological activity of both IL-4 and IL-13. The binding of one cytokine did not alter affinity for the other cytokine.[15] In mouse models of immune activation in response to immunization and challenge with ovalbumin, IL-4 blockade reduced late-phase ear swelling and IgE production, and IL-13 blockade reduced airway hyper-responsiveness, lung eosinophilia, serum chitinase levels and chemokine gene expression. The bifunctional IL-4/IL-13 antagonist effectively blocked all responses.[15] These findings demonstrate that a bifunctional molecule that recognizes mouse IL-4 and IL-13 could effectively target both cytokines *in vivo*.

The current study aimed to evaluate the efficacy and potency of a biotherapeutic targeting both IL-4 and IL-13 in a mouse model of oxazolone-induced UC. The bifunctional antagonist reduced body-weight loss throughout the 7-day course of the study, reduced overall disease activity, and counteracted the decreased colon length that accompanies disease. Furthermore, use of this bifunctional IL-4/IL-13 antagonist revealed a panel of effective biomarkers indicative of IL-4/IL-13 pathway activation in this model.

Materials and methods

Construction of murine anti-mouse IL-4 antibody

Heavy-chain and light-chain variable regions (V_H and V_L, respectively) were cloned from rat 11B11 hybridoma cells (American Type Culture Collection; ATCC, Manassas, VA) using the SMART cDNA synthesis system (Clontech Laboratories Inc, Mountain View, CA) followed by PCR amplification. The V_H and V_L sequences were sub-cloned into the pSMED2-mouse IgG1 and pSMEN3-mouse κ expression vectors, respectively, to construct the 11B11-mouse IgG1/κ version of this antibody (mu11B11 mAb). DNA was transiently transfected into COS-1 (M6) cells, using a TransIT (Mirus Bio LLC, Madison, WI)/Opti-MEM system (Gibco; Invitrogen Life Technologies, Carlsbad, CA), and maintained in Dulbecco's modified Eagle's medium containing 10% heat-inactivated fetal bovine serum, 100 IU penicillin, 100 μg/ml streptomycin and 2 mM glutamine, in a 37° incubator at 10% CO_2.

Generation of murine bifunctional IL-4/IL-13 antagonist

The mouse bifunctional IL-4/IL-13 antagonist consists of mouse sIL-13Rα2-Fc, mouse C57BL/6 IgG2c Fc domain lacking the C-terminal lysine residue,[16] a linker sequence, anti-mouse IL-4 mu11B11 V_L, a minimal 16 amino acid glycine–serine linker, and anti-mouse IL-4 mu11B11 V_H. DNA fragments encoding these components were generated by PCR amplification of gene-specific DNA templates with VENT polymerase (New England Biolabs, Ipswich, MA) using appropriate oligonucleotide primers (Integrated DNA Technologies, Coralville, IA). CHO PA-Dukx 153.8 cells were stably transfected with DNA encoding the bifunctional antagonist using TransIT (Mirus Bio LLC)/Opti-MEM (Gibco; Invitrogen). Concentrated conditioned medium was loaded onto Protein A–Sepharose Fast Flow (Invitrogen), washed with PBS pH 7·2, and bound protein was eluted with 20 mM citric acid, 150 mM NaCl, pH 2·5. Material was immediately neutralized with 5% 2 M Tris–HCl pH 8·0, then loaded onto a Superdex 200 column to remove aggregates. The final pool was analysed by optical density at 280 nm, endotoxin assay, protein A ELISA, analytical size exclusion and SDS/IEF PAGE. The material (180 000 molecular weight) was formulated in Ca^{2+}, Mg^{2+}-free PBS, pH 7·2 (CMF-PBS).

Measurement of bifunctional antagonist concentration in serum

ELISA plates (MaxiSorp; Nunc, Rochester, NY) were coated with anti-FLAG M2 (Sigma Aldrich, St Louis,

MO) in PBS. Plates were blocked with 0·5% gelatin in PBS, and washed in PBS containing 0·05% Tween-20 (PBS-Tween). Standard dilutions of bifunctional antagonist or serum samples were added, along with a mixture of human IL-13 FLAG (Pfizer Global Research and Development; PGRD, Cambridge, MA) and murine IL-4 (R&D Systems, Minneapolis, MN). Plates were incubated at room temperature for 4 hr then washed with PBS-Tween. Biotinylated goat anti-mouse IL-4 (R&D Systems) was added and incubated for 2 hr at room temperature. Plates were washed with PBS-Tween, and binding was detected with peroxidase-linked streptavidin (SouthernBiotech, Birmingham, AL) and Sure Blue substrate (KPL Inc, Gaithersburg, MD). The reaction was stopped with 0·01 M sulphuric acid, and absorbance was read at 450 nm in a SpectraMax plate reader (Molecular Devices, Sunnyvale, CA). The lower limit of quantification of the assay was 2 ng/ml bifunctional antagonist.

STAT6 phosphorylation assay

The murine Ba/F3 pro-B cell line (ATCC), which expresses IL-4Rα and γ common receptor chains, was transfected with murine IL-13Rα1 to generate a line responsive to IL-13 in addition to IL-4. Cells were challenged with 1 ng/ml IL-13 or 0·5 ng/ml IL-4 in the presence or absence of antagonist at 37° for 30 min, washed into ice-cold PBS containing 1% BSA, then fixed in 1% paraformaldehyde for 15 min at 37°. To permeabilize the nucleus, cells were incubated overnight at −20° in absolute methanol, washed into PBS-BSA, then stained with AlexaFluor 488-labelled antibody to STAT6 (pY641; BD Biosciences, San Jose, CA). Fluorescence was analysed with a FACSCalibur (BD Biosciences), and FLOWJO software version 7.2.4 (Tree Star Inc, Ashland, OR).

ELISA for acute-phase proteins

The concentration of serum amyloid P (SAP) was determined in sera from end bleeds using a commercially available ELISA from Kamiya Biomedical Company (Seattle, WA), following the manufacturer's recommended procedures. SAP was assayed in sera that had been stored at −80°, and diluted at 1 : 30 000. The concentration of analyte in each diluted sample was determined from the measured absorbance at 450 nm by interpolation from a standard curve.

Mouse oxazolone-induced colitis model

Studies were conducted by Invitek Corp (San Francisco, CA). All animal studies were performed in accordance with the National Institutes of Health Guide for the Care and Use of Laboratory Animals. All work was conducted according to Invitek Standard Operating Procedures, and

in accordance with the Pfizer Animal Care and Use Policy. After at least 7 days of acclimatization, mice were grouped according to their body weight. Each treatment group consisted of 15 SJL/J female mice (Jackson Laboratory, Bar Harbor, ME), 7–8 weeks of age, weighing 18–20 g. Mice were pre-sensitized under light anaesthesia with a ketamine (80–120 mg/kg) and xylazine (5–10 mg/kg) cocktail. A small area of dorsal skin was shaved and approximately 200 µl of 3% (weight/volume) solution of oxazolone (4-ethoxymethylene-2-phenyl-2-oxazoline-5-one; OXA) in 100% ethanol was applied. After 5 days of pre-sensitization, mice were challenged intra-rectally with 150 µl of 1% oxazolone in 50% ethanol under light anaesthesia with ketamine/xylazine. One group of mice was sensitized and challenged with OXA, but was given no treatment (OXA group). Treatment groups were administered bifunctional antagonist, IL-13 blocker (sIL-13Rα2-mouse IgG2aFc), anti-IL-4 (murine 11B11), or mouse IgG2a control, intraperitoneally, at the indicated doses in saline. A separate control group of six mice was pre-sensitized with 200 µl of 100% ethanol containing no oxazolone (no OXA control group), and did not develop disease. Dosing solutions were prepared in freshly sterile-filtered PBS. The test substances were administered intraperitoneally once every 2 days, beginning 1 day before the intrarectal challenge (days −1, 1, 3, 5 and 7) for a total of five doses. Exactly 24 hr post final dose, all surviving mice were killed using CO_2 asphyxiation and serum was collected and immediately stored at −70°.

Measurement of body weights and disease activity index

Body weights were measured before intrarectal administration of oxazolone on day 0 and daily thereafter for 7 days using a calibrated laboratory balance. The parameters used for clinical assessment using a disease activity index are shown in Fig. 2(b) and were a composite score based on body weight, stool consistency and the presence of blood in the stools. Stool consistency was observed visually and occult/gross bleeding was measured using a Beckman Coulter occult blood testing kit (Brea, CA). Disease activity index (DAI) scores for animals that died before study termination were excluded from analysis.

Tissue harvest, RNA preparation and gene expression analysis

At study termination, mice were killed by CO_2 asphyxiation and colons (including caecum) were removed. Colon lengths and weights were taken (excluding caecum and all faecal matter). The colons (including caecum) were cleaned of all faecal matter with PBS. The inflamed colon was isolated as the portion spanning approximately 6 cm proximal to anus, placed in RNA-later (Catalog No. 76106; Qiagen, Valencia, CA) and immediately frozen in

liquid nitrogen. RNA was prepared from 350 μl of colon homogenate using RNeasy Mini reagents and a QIAcube fully automated sample prep system (Qiagen). RNA quality was assessed by the integrity of 28S and 18S peaks on the Agilent 2100 Bioanalyzer (Agilent Technologies, Santa Clara, CA) and quantified by spectrophotometry at 260 and 280 nm on a Nanodrop 2000 (Thermo Scientific, Wilmington, DE). A_{260}/A_{280} ratios were also used as an additional assessment of RNA quality. A high-capacity cDNA Synthesis kit (Applied Biosystems, Foster City, CA) was used to generate cDNA. For each low density array reaction, 100 ng of RNA was converted to cDNA in a 10-μl total reaction volume. Following cDNA synthesis, 10 μl of the total reaction was combined with 40 μl of water and 50 μl of Taqman Gene Expression Master Mix (Applied Biosystems). Taqman low density array cards were loaded and run on a 7900HT Real-Time PCR System (Applied Biosystems). Expression levels were normalized to control genes across all samples and relative quantification values were calculated in relation to an average of the 'no oxazolone' control subset using SPOTFIRE DECISIONSITE 9.0 (TIBCO, Somerville, MA). Gene expression differences between individual groups were compared and Welch Test statistical analysis was applied.

Statistical analysis

For analysis of colon length, colon weight and DAI at death, treatment groups were compared with the mouse IgG2a-treated control group, and *P*-values were determined by unpaired two-tailed Student's *t*-test, with normality determined by D'Agostino–Pearson omnibus test. For analysis of body weight changes over the course of disease, treatment groups were compared with the IgG2a

control group by two-way analysis of variance. Survival was analysed using Kaplan–Meier curves, and differences between the groups were determined by Mantel–Cox log rank test. All analysis was performed using GRAPHPAD PRISM software, version 6 (GraphPad Software Inc, La Jolla, CA).

Results

Generation and characterization of murine IL-4/IL-13 bifunctional antagonist

A bifunctional molecule with specificity for murine IL-4 and IL-13 was produced on a multi-specific protein therapeutic platform (Emergent BioSolutions, Rockville, MD), as described previously.[15] The N-terminus of the molecule consisted of an IL-13-binding domain derived from the murine IL-13Rα2 extracellular sequence, linked to the C57BL/6 IgG2c Fc. This was connected through a linker sequence to a C-terminal IL-4-binding domain, comprised of the scFv generated from CDR sequences of the rat anti-mouse IL-4 mAb 11B11[17] (Fig. 1a). A schematic of the bifunctional IL-4/IL-13 antagonist is shown in Fig. 1(b). Binding data indicated binding of two molecules of IL-13 but only one molecule of IL-4 per molecule of bifunctional antagonist.[15] In a STAT6 phosphorylation bioassay in mouse Ba/F3 cells transfected with IL-13Rα1 and IL-4Rα, the bifunctional antagonist effectively inhibited bioactivity of both murine IL-4 and IL-13. The activity against IL-4 was reduced compared with that of purified mAb 11B11, and the activity against IL-13 was comparable to that of sIL-13Rα2-Fc (Fig. 1c). Overall, the bifunctional antagonist had approximately 20-fold lower potency in a cell-based assay against IL-4 compared with
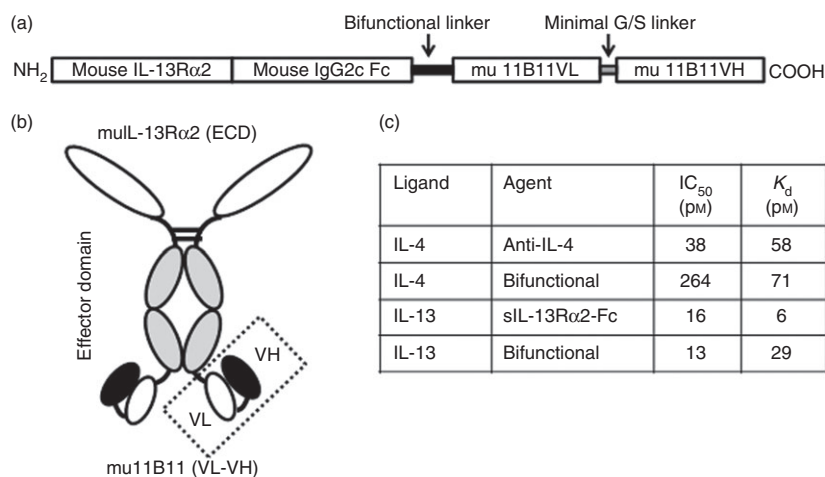

Figure 1. Schematic of murine interleukin-4 (IL-4/IL-13 dual antagonist. (a) Configuration of IL-4/IL-13 dual antagonist, from N-terminal mouse IL-13Rα2 extracellular domain (ECD) to C-terminal scFv of anti-mouse IL-4 monoclonal antibody (mAb) mu11B11. (b) Schematic indicating overall structure of the IL-4/IL-13 dual antagonist, with two binding sites for each cytokine. (c) Cell-based IC_{50} and SPR-derived K_d values for anti-mouse IL-4 mAb mu11B11, sIL-13Rα2-Fc, and bifunctional IL-4/IL-13 antagonist. IC_{50} values were derived from a signal transducer and activator of transcription 6 (STAT6) phosphorylation bioassay using BaF3 cells expressing murine IL-13Rα1 and IL-4Rα.

IL-13. The bifunctional molecule had a serum half-life of approximately 4·7 days in C57BL/6 mice.[15]

Effect on disease end-points in oxazolone-induced colitis model

A schematic outline of the oxazolone-induced colitis model is shown in Fig. 2(a). To induce disease, mice were pre-sensitized with a solution of OXA in 100% ethanol, painted onto the skin daily for 5 days, as described in the Materials and methods. After 5 days of pre-sensitization, mice were challenged intrarectally with OXA in 50% ethanol daily for 8 days (days 0–7). A control group of mice was sensitized and challenged with ethanol in the absence of oxazolone (no OXA control). Study drug was administered intraperitoneally every other day, starting 1 day before the intra-rectal challenge (days −1, +1, +3, +5, and +7). Animals were monitored daily for signs of disease, as summarized in the DAI (Fig. 2b). On killing,

(a) Oxazolone-induced colitis model
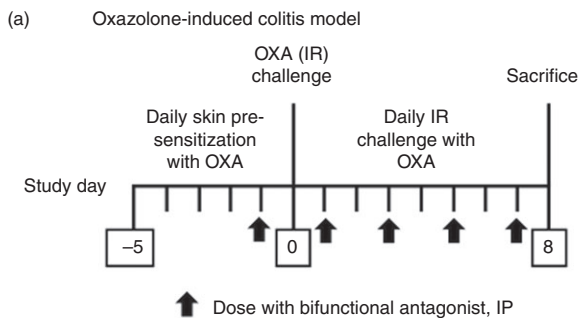
(b) Disease activity index

Score	Body weight loss (%)	Stool consistency	Occult/Gross bleeding
0	No loss	Normal	Normal
1	1–5	Loose	Occult
2	5–10	Loose	Occult
3	10–15	Loose	Occult
4	> 15	Diarrhoea	Gross bleeding

Figure 2. (a) Schematic representation of oxazolone-induced colitis model. Female SJL/J mice were sensitized with oxazolone painted on the skin daily for 5 days, then challenged intrarectally with oxazolone daily starting on Day 0. Starting the day before intrarectal challenge (Day −1) and every other day, mice were administered protein therapeutics intraperitoneally. At time of killing on Day 8, colons were excised and length and weight were determined. (b) Disease activity index. The daily clinical assessment was performed after the intrarectal oxazolone challenge. Stool consistency was observed visually and occult/gross bleeding was assessed using the Beckman Coulter occult blood testing kit.

colons were excised, photographed and measured for length and weight. Disease severity was associated with a reduction in colon length and increase in colon weight.

The bifunctional IL-4/IL-13 antagonist, administered at doses of 8, 2, or 0·5 mg/kg, had efficacy in the model (Fig. 3). It reduced body weight loss throughout the 7-day course of disease (Fig. 3a), maintained colon length (Fig. 3b,d), minimized gains in colon weight (Fig. 3c), ameliorated the increase in colon weight/colon length ratio (Fig. 3e), and reduced overall DAI (Fig. 3f). Although the three doses of bifunctional antagonist showed comparable activities, within the limits of quantitative discrimination afforded by the model, there appeared to be a reverse dose dependence in the body weight (Fig. 3a) and DAI (Fig. 3f) end-points.

Effects of the bifunctional molecule were compared with those of single cytokine blocking agents, anti-mouse IL-4, and the IL-13 antagonist, sIL-13Rα2-Fc. Both anti-IL-4 and the bifunctional antagonist showed efficacy in modulating body weight loss (Fig. 4a) and counteracting the reduction in colon length (Fig. 4b). Although effects of the sIL-13Rα2-Fc activity failed to reach statistical significance in this study, there was a trend toward efficacy on moderation of colon length (Fig. 4b), and on body weight loss on days 4–7 (Fig. 4a). None of these agents had a significant effect on mortality in this model (Fig. 4c).

Proportional neutralization of IL-4 and IL-13 by the bifunctional antagonist

As summarized in Fig. 1, the bifunctional IL-4/IL-13 antagonist effectively inhibited the bioactivity of murine IL-4 and IL-13 cytokines in the STAT6 phosphorylation bioassay. To evaluate the relative IL-4 and IL-13 neutralization capacity in the circulation of treated mice, we examined the ability of serum from treated animals to inhibit the STAT6 phosphorylation response of IL-13Rα1/IL-4Rα-expressing BaF3 cells in response to limiting concentrations of exogenously added IL-4 or IL-13. Interleukin-4 neutralization was assayed at a serum dilution of 1 : 20, and IL-13 neutralization at a dilution of 1 : 300, consistent with the relatively lower potency of the bifunctional molecule against IL-4 compared with IL-13. When these values were normalized for relative potency against each cytokine, results showed that the bifunctional molecule reduced the bioactivity of IL-4 and IL-13 proportionally (Fig. 5a), and that the relative amount of IL-4 and IL-13 neutralization activity was directly related to serum titres of the dual antagonist (Fig. 5b).

Serum SAP concentration is associated with disease severity

Because elevations in the serum amyloid proteins SAA and SAP have been reported in mouse colitis models,[18,19]
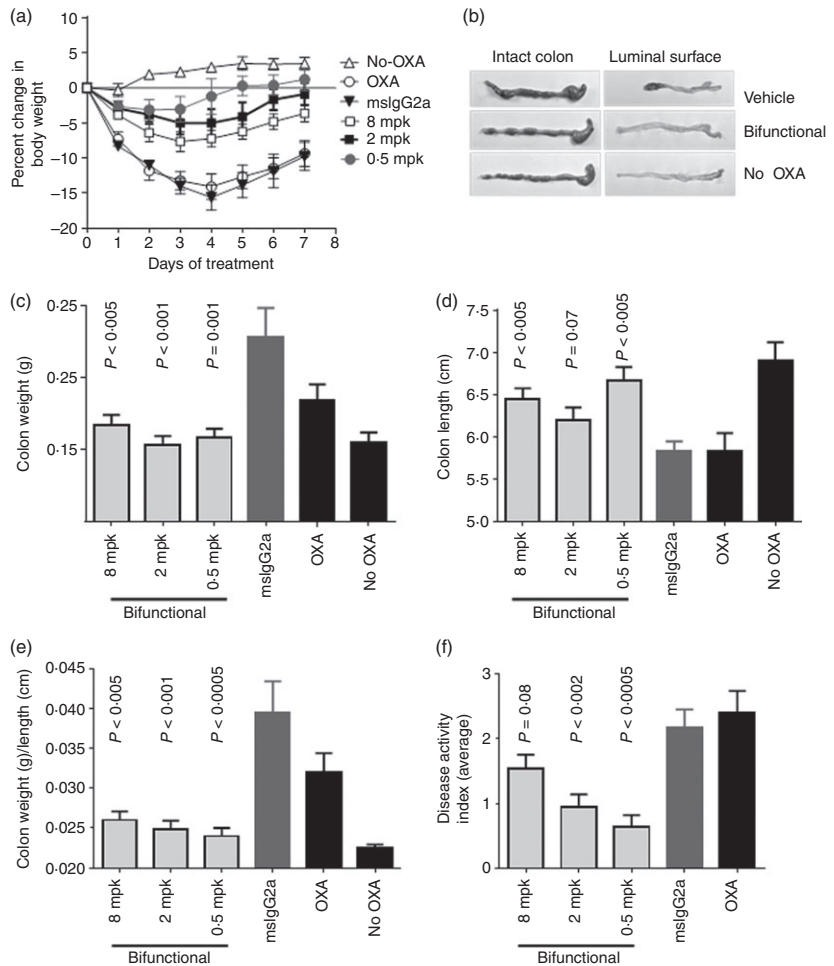
Figure 3. Activity of bifunctional interleukin-4 (IL-4)/IL-13 antagonist in oxazolone-induced colitis model. Groups of 15 female SJL/J mice were sensitized with oxazolone painted on the skin on Day −5, then challenged intrarectally with oxazolone on Day 0. Starting the day before intrarectal challenge (Day −1), mice were administered bifunctional antagonist at 8, 2, or 0·5 mg/kg intraperitoneally, every 2 days. Control animals were given oxazolone but no treatment (OXA), were given OXA and treated with mouse IgG2a control, or had no disease induction (no OXA). (a) On Days 1–7, the animals were scored for body weight. At time of killing on Day 8, colons were excised. (b) Morphology of colons at death. Representative colons are shown from animals given OXA but no treatment (OXA), those given OXA and treated with bifunctional IL-4/IL-13 antagonist (8 mg/kg) or animals that had no disease induction (no OXA). (c) Colon weight, (d) colon length; (e) ratio of colon weight/length; and (f) disease activity index (average over the 7-day study) are shown as indicators of disease severity. *P*-values were determined by *t*-test in comparison with the mouse IgG2a-treated control group.

SAP concentration was assayed in serum. The concentration of serum SAP was elevated with oxazolone administration, and was inversely proportional to body weight (Fig. 6a) and colon length (Fig. 6b), indicating an association with active disease. Serum concentrations of the bifunctional molecule were assayed in end bleeds of treated mice. Concentrations recovered in the serum were proportional to dose administered to the mice. Figure 6(c) shows an inverse relationship between serum concentrations of bifunctional IL-4/IL-13 antagonist and colon length, consistent with an effect on disease severity. Reduced serum SAP concentration was seen in animals treated with bifunctional antagonist, in proportion to the antagonist titre in end bleeds (Fig. 6d). Similar findings were seen for SAA (data not shown).

Effects of IL-4/IL-13 bifunctional antagonist on colon gene expression

To assess biomarkers reflective of IL-4 and/or IL-13 biology within the inflamed colon, gene expression analysis was performed with colon tissue. Anti-IL-4, sIL-13Rα2-Fc, and the bifunctional IL-4/IL-13 antagonist all affected the expression of several genes associated with inflammation in the colon. Relative gene expression was calculated using the untreated control group as the comparator. Expression of a panel of genes was found to correlate with markers of disease severity, including colon length (Fig. 7). A set of genes was identified that was significantly changed by the bifunctional molecule across several experiments. Gene expression patterns were related to the amount of antagonist that was detectable in the sera from end bleeds of the individual animals (Fig. 8). These findings support the dose-dependent modulation of disease activity with bifunctional IL-4/IL-13 antagonist.

Discussion

A bispecific immunotherapeutic targeting murine IL-4 and IL-13 was generated on a novel multi-specific protein therapeutic scaffold. The molecule consists of N-terminal IL-13-binding domains derived from the murine sIL-13Rα2 extracellular region, linked to murine IgG2c Fc, followed at the C-terminus by scFv domains targeting IL-4, derived from the anti-mouse IL-4 mAb, 11B11. The bifunctional IL-4/IL-13 antagonist potently binds to and
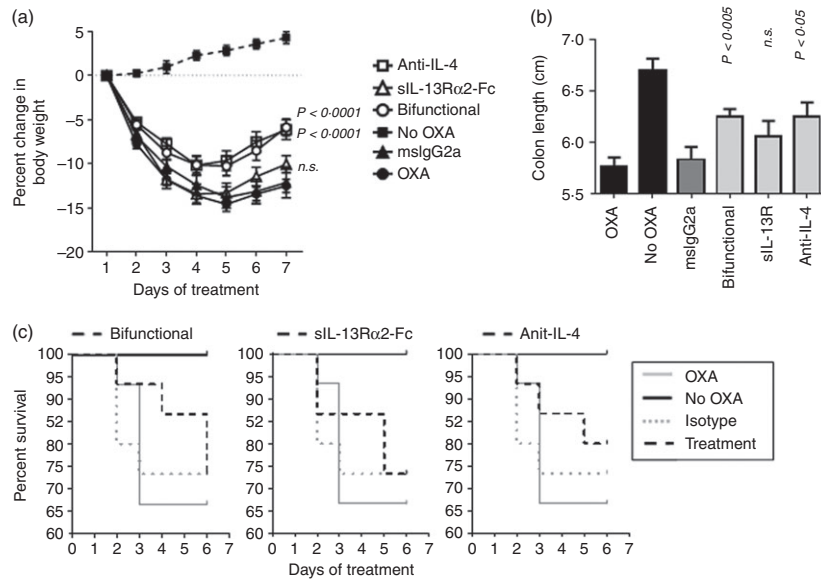
Figure 4. Activity of anti-interleukin-4 (IL-4), sIL-13Rα2-Fc and bifunctional IL-4/IL13 antagonist (3 mg/kg) in oxazolone-induced colitis. Female SJL/J mice were sensitized and challenged with oxazolone as described above. Starting the day before intrarectal challenge (Day −1), mice were given the protein therapeutics at 3 mg/kg intraperitoneally, every 2 days. Control animals were given oxazolone but no treatment (OXA), were given OXA and treated with mouse IgG2a control, or had no disease induction (no OXA). The no OXA group contained six animals. All other groups contained 15 animals on day 0. (a) Body weight throughout the course of treatment. *P*-values were determined by two-way analysis of variance in comparison with the mouse IgG2a-treated control group. (b) Colon length at time of death. *P*-values were determined by *t*-test in comparison to the mouse IgG2a-treated control group. (c) Kaplan–Meier curves, showing % survival throughout the course of treatment. In separate panels, survival of treatment groups is plotted in relation to the OXA, no OXA, and mouse IgG2a control groups; bifunctional antagonist (left), sIL-13Rα2-Fc (middle), anti-IL-4 (right). There were no statistically significant differences in survival between mice in these groups and those given mouse IgG2a control, as determined by Mantel–Cox log rank test.
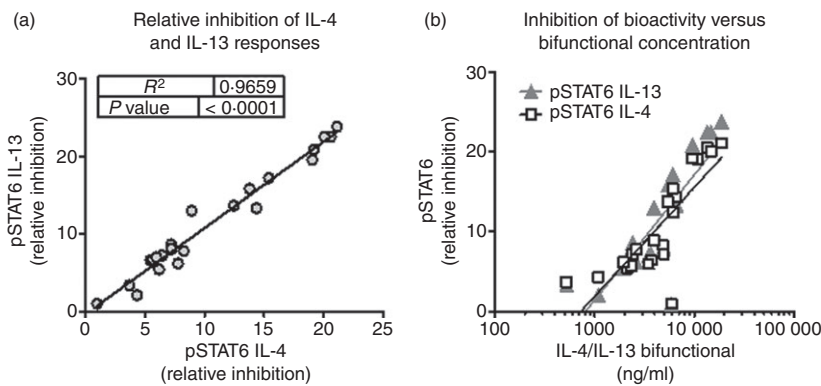

Figure 5. Interleukin-4 (IL-4) and IL-13 neutralization capacity in sera of mice from oxazolone-induced colitis model is proportional to serum concentration of bifunctional antagonist. Female SJL mice were sensitized and challenged with oxazolone as described above. Starting the day before intrarectal challenge (Day −1), mice were administered bifunctional IL-4/IL-13 antagonist at 3 or 8 mg/kg intraperitoneally, every 2 days. On Day 8, sera were collected and titres of antagonist were measured by ELISA. BaF3 cells expressing IL-4 and IL-13 receptors were incubated with sub-optimal concentrations of murine IL-4 or IL-13, in the presence of serum dilutions, for 30 min at 37°. Cells were fixed, permeabilized and stained for expression of phosphorylated signal transducer and activator of transcription 6 (STAT6). The presence of IL-4 or IL-13 neutralization activity in the sera reduced the STAT6 phosphorylation response to exogenous murine IL-4 or IL-13. (a) The relative IL-4 or IL-13 neutralization activity of individual serum samples was evaluated as the per cent inhibition of the pSTAT6 response, corrected for serum dilution. The relative potency of IL-4 and IL-13 neutralization was proportional. (b) IL-4 or IL-13 neutralization activity, plotted as a function of serum titer of IL-4/IL-13 antagonist.

neutralizes both cytokines, and was used to establish proof of concept for efficacy of the bifunctional strategy in mouse models of inflammation. Previous studies have shown that the bifunctional molecule effectively targets both cytokines. In a murine model of lung inflammation following immunization and airway challenge with oval-

Figure 6. Serum concentrations of serum amyloid P (SAP) are associated with disease activity in the oxazolone-induced colitis model. Female SJL mice were sensitized and challenged with oxazolone. Starting the day before intrarectal challenge (Day −1), mice were administered bifunctional interleukin-4 (IL-4)/IL-13 antagonist, at 8, 3, or 0·5 mpk every 2 days. At time of killing on Day 7, sera were collected and assayed for SAP by ELISA. Associations between these readouts and disease correlates are shown for all animals in the study, across all treatment groups: (a) average body weight versus serum SAP; (b) colon length versus serum SAP; (c) serum bifunctional IL-4/IL-13 antagonist concentration versus colon length; (d) serum concentrations of bifunctional IL-4/IL-13 antagonist versus SAP for the 0·5 mpk dose group. R^2 and P-values were derived from linear regression analysis.
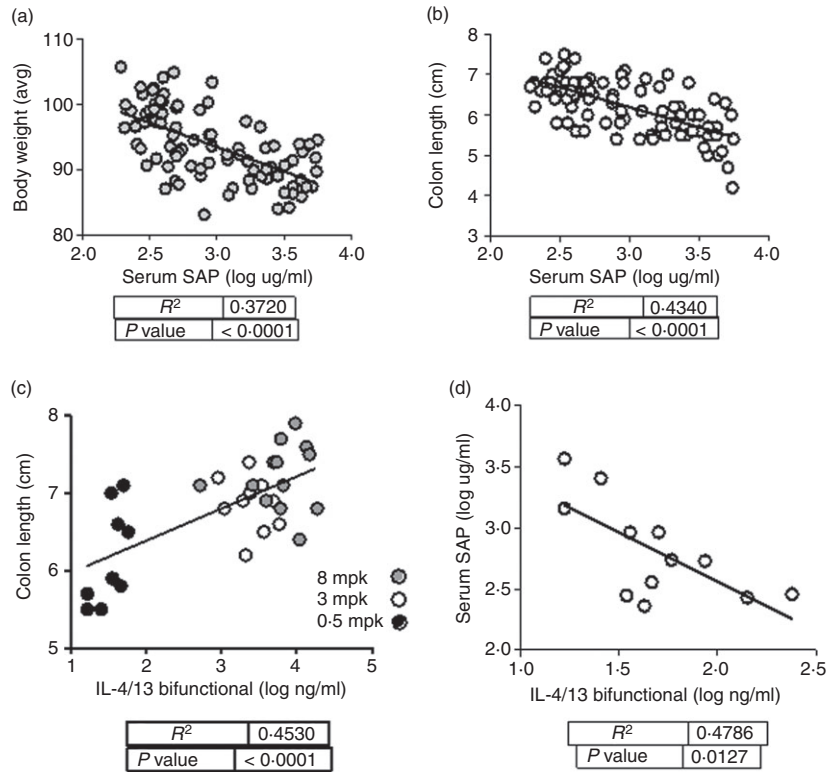
bumin, the bifunctional antagonist reduced all inflammatory responses to IL-4 and IL-13.[15] The current study uses this novel modality to test the efficacy of IL-4/IL-13 blockade in a mouse model of colitis. Although it is based on the immunoglobulin scaffold, the bifunctional antagonist described here is a novel protein construct, with a half-life of 4·7 days in the mouse.[15] While *in vivo* neutralization, anti-drug antibodies, and other mechanisms of depletion were not apparent in the short-term disease model described here, further studies will be required to confirm that this type of molecule can be used with chronic dosing paradigms to treat ongoing disease.

Like human UC, the oxazolone-induced colitis model is thought to be Th2-driven. Both IL-4 and IL-13 may contribute to intestinal inflammation and disease pathogenesis, through several potential mechanisms. Interleukin-4 has been reported to reduce transepithelial resistance in monolayers of intestinal epithelial cells.[6] Similarly, IL-13 can compromise transepithelial resistance and lead to permeabilization of the epithelial barrier through epithelial cell apoptosis and disruption of tight junctions.[4,20] By elevating expression of the tight junction paracellular pore component, claudin-2, IL-13 may also promote ion flux across the barrier.[21,22] In parasite infection models, both IL-4 and IL-13 have been found to influence goblet cell hyperplasia,[23–25] eotaxin expression in colonic mucosa[26] and smooth muscle hypercontractility[27,28] in the gut. Interleukin-13 is a potent inducer of tissue fibrosis,[29] has been associated with fibrotic changes in

fistulas of inflammatory bowel disease (IBD),[30] and represents a promising therapeutic target for the treatment of colitis.[31]

Adoptive transfer studies have established that IL-4-producing CD4+ T cells can mediate disease induction in the oxazolone-induced colitis model, and that production of IL-13 by these cells drives pathology.[32] Interleukin-4 can also be produced by lesional infiltrating T cells, and anti-IL-4 antibody 11B11 reduced disease severity in oxazolone-induced colitis.[10] Secretion of Th2 cytokines (IL-4, IL-5, and IL-13) from lesional infiltrating T cells can be modulated by additional anti-inflammatory treatments, including FTY-720 and dexamethasone.[33] In mice deficient in CD30L[34] or calcitonin gene-related peptide[35], exacerbated disease was accompanied by enhanced secretion of IL-4, IL-5 and IL-13 from lamina propria T cells.[34,35] Colitis in CD30L-deficient mice could be effectively treated with anti-IL-4 antibody 11B11,[34] further validating the critical role of Th2 cytokines in this disease model.

Other studies have implicated natural killer T cells as the source of IL-13 in this model, and demonstrated the therapeutic activity of neutralizing IL-13 with sIL-13Rα2-Fc,[3] or reducing its production following treatment with antibodies to IL-25 or the IL-25 receptor, IL-17BR.[36] Invariant natural killer T cells, capable of producing both IL-4 and IL-13, have been associated with the greater disease susceptibility of germ-free mice compared with specific pathogen-free mice in the oxazolone-induced colitis model.[37] Furthermore, recent studies have implicated IL-4
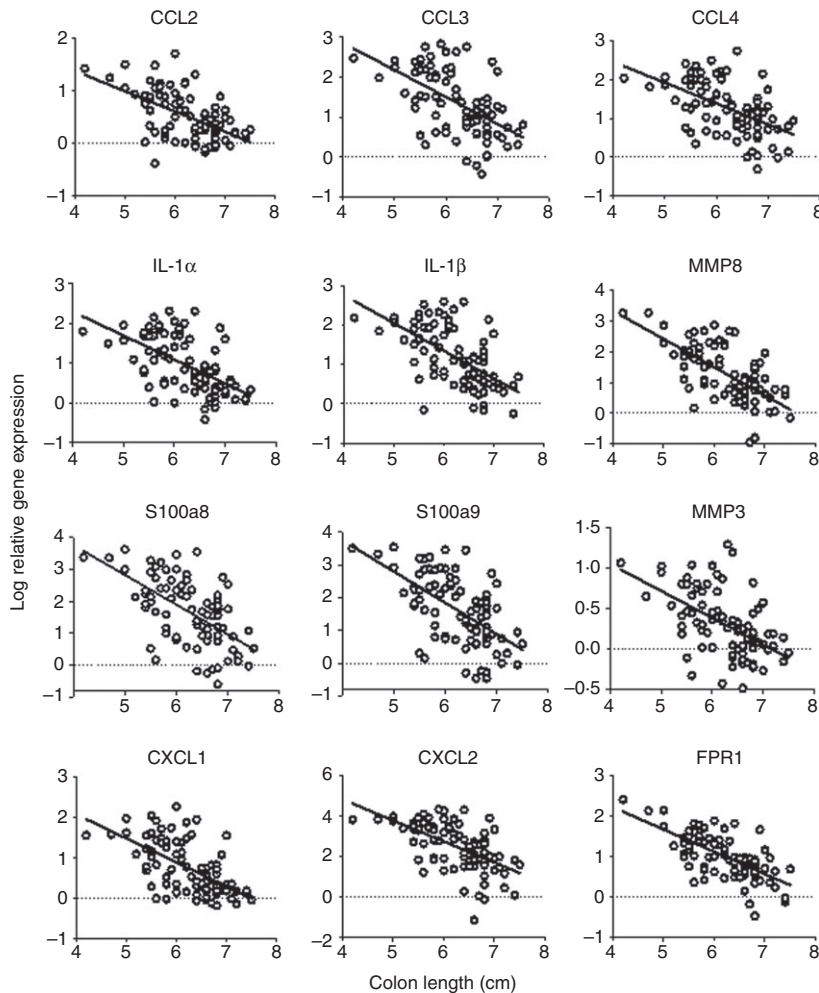
Figure 7. Colon gene expression changes associated with disease severity. Gene expression data were plotted as a function of colon length for individual animals, with shorter colon indicative of more severe disease. In each case, $P < 0.0001$ for the correlation.

in mediating exacerbation of colitis induced by IL-33, suggesting that IL-33 triggers induction of IL-4.[38]

Mice lacking IL-4Rα[32] or those deficient in STAT6,[39] are unable to respond to either IL-4 or IL-13, and do not develop disease in the oxazolone-induced colitis model, further supporting the critical role of these cytokines. By targeting the receptor chain or signalling pathway shared by IL-4 and IL-13, these studies have shown the potential for disease amelioration by modulation of the common pathway, but relied on genetic depletion of IL-4Rα or STAT6. This carries the potential for developmental impacts that may not be mimicked therapeutically. Our study is the first to examine the effects of simultaneous IL-4 and IL-13 blockade in intact animals using a therapeutic intervention. Furthermore, because IL-4Rα is widely expressed on fibroblasts, epithelial cells, endothelial cells, lymphocytes and other cell types, and STAT6 is an intracellular target that has yet to be effectively blocked therapeutically, targeting trace amounts of cytokine offers a potential advantage in terms of efficiency of target engagement and coverage.

Because the oxazolone-induced colitis model does not support a high degree of quantitative differentiation between treatment paradigms, we could not confirm that dual blockade of IL-4 and IL-13 had enhanced potency over inhibition of either cytokine alone. Nevertheless, studies of the same bifunctional antagonist in a model of ovalbumin-induced lung inflammation did support the greater potency of dual cytokine blockade.[15] In the current study, the simultaneous targeting of IL-4 and IL-13 with the bifunctional molecule allowed us to examine a range of biomarkers affected by disruption of the Th2 pathway in this disease. These biomarker changes allow quantitative associations to be drawn between the degree of response and relative exposure, measured as concentration of antagonist in end bleeds. We observed changes in SAP in mice treated with bifunctional IL-4/IL-13 antagonist, with the magnitude of effect found to be inversely related to that of antagonist. Elevated serum concentrations of the acute-phase proteins SAA and SAP have been reported in mouse colitis models.[18,19] In human IBD, the acute phase C-reactive protein is associated with Crohn's disease, but appears less related to the inflammatory response of UC.[40,41] Our findings suggest that serum concentration of SAP could be an informative biomarker of disease severity in the oxazolone-induced colitis model in mice.
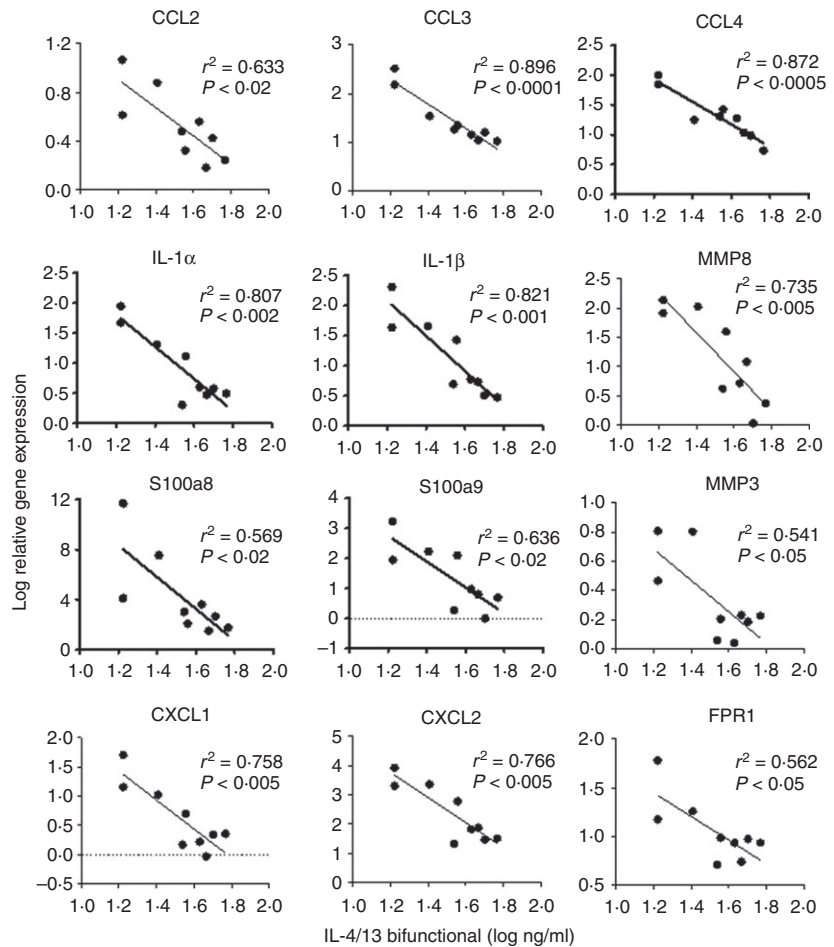
Figure 8. Colon gene expression changes are proportional to serum concentration of bifunctional interleukin-4 (IL-4) /IL-13 antagonist. Gene expression data were plotted against the concentration of bifunctional antagonist in the serum for individual animals given a 0·5 mg/kg dose. R^2 and P-values are shown as measures of correlation and significance.

Similarly, changes in expression of numerous tissue-associated genes were seen in mice treated with bifunctional IL-4/IL-13 antagonist, and the degree of gene modulation was proportional to serum concentration of the therapeutic in the end bleeds. This group of genes included the chemokines Ccl2 (MCP-1), Ccl3 (MIP-1α), Ccl4 (MIP-1β), Cxcl1 (Gro-α), and Cxcl2 (MIP-2), the cytokines IL-1α and IL-1β, a formyl peptide receptor (Fpr1), the matrix metalloproteases Mmp3 and Mmp8, and the calprotectin subunits S100a8 and S100a9. Several of these markers have been found to be elevated in IBD,[42–45] and both Mmp-3[46] and Mmp-8[47] transcripts are associated with UC. Expression of the calprotectin protein (S100a8/a9) in sera, mucosal or fecal samples is a biomarker for human IBD diagnosis, activity, or relapse,[48] and the S100a9 gene is over-expressed in inflamed colon tissue of human UC and Crohn's disease.[49] The increased expression of these genes is consistent with disease activity in oxazolone-induced colitis, and helps to validate the therapeutic activity of IL-4/IL-13 blockade at the site of inflammation.

The quantitative limitations of this model made it difficult to evaluate the dose responses seen with the bifunctional antagonist. In some readouts, including body weight loss (Fig. 3a) and DAI (Fig. 3f), there appeared to be a reverse dose dependence, with the 0·5 mg/kg dose showing greater activity than the 8 mg/kg dose. In other readouts, including serum SAP (Fig. 6d) and gene expression (Fig. 8), the magnitude of change was directly proportional to the circulating concentration of antagonist. Although these findings most likely reflect variations due to the relatively small therapeutic window seen in this model, we cannot rule out a biological rationale. In a recent phase 2b asthma study, anti-IL-13 lebrikizumab appeared to display a reverse dose response for modulation of exacerbation rate.[50] Future studies will further explore the dose dependence of Th2 modulation in these systems.

Taken together, these findings support the involvement of IL-4 and IL-13 in oxazolone-induced colitis, a murine model of UC. IL-13 antibodies are being developed for treatment of colitis,[31] and a role for IL-4 is beginning to be appreciated. Recent reports that IL-13 blockade had only limited efficacy in human UC studies[51,52] emphasize the potential importance of neutralizing the shared effector activities mediated by IL-4 along with IL-13. Use of the bifunctional IL-4/IL-13 antagonist has allowed us to confirm the efficacy of dual cytokine blockade in a mouse

model of colitis, and to define a panel of biomarkers quantitatively associated with IL-4/IL-13 pathway inhibition. Where both agents are known to be involved, bifunctional targeting presents a novel and promising therapeutic option.

Disclosures

The authors declare no conflicts of interest.

References

1 Kasaian MT, Miller DK. IL-13 as a therapeutic target for respiratory disease. *Biochem Pharmacol* 2008; **76**:147–55.

2 Inoue S, Matsumoto T, Iida M, Mizuno M, Kuroki F, Hoshika K, Shimizu M. Characterization of cytokine expression in the rectal mucosa of ulcerative colitis: correlation with disease activity. *Am J Gastroenterol* 1999; **94**:2441–6.

3 Heller F, Fuss IJ, Nieuwenhuis EE, Blumberg RS, Strober W. Oxazolone colitis, a Th2 colitis model resembling ulcerative colitis, is mediated by IL-13-producing NK-T cells. *Immunity* 2002; **17**:629–38.

4 Heller F, Florian P, Bojarski C et al. Interleukin-13 is the key effector Th2 cytokine in ulcerative colitis that affects epithelial tight junctions, apoptosis, and cell restitution. *Gastroenterology* 2005; **129**:550–64.

5 Olsen T, Cui G, Goll R, Husebekk A, Florholmen J. Infliximab therapy decreases the levels of TNF-α and IFN-γ mRNA in colonic mucosa of ulcerative colitis. *Scand J Gastroenterol* 2009; **44**:727–35.

6 Berin MC, Yang PC, Ciok L, Waserman S, Perdue MH. Role for IL-4 in macromolecular transport across human intestinal epithelium. *Am J Physiol* 1999; **276**(5 Pt 1):C1046–52.

7 Mannon PJ, Hornung RL, Yang Z et al. Suppression of inflammation in ulcerative colitis by interferon-β-1a is accompanied by inhibition of IL-13 production. *Gut* 2010; **60**:449–55.

8 Kojima R, Kuroda S, Ohkishi T, Nakamaru K, Hatakeyama S. Oxazolone-induced colitis in BALB/C mice: a new method to evaluate the efficacy of therapeutic agents for ulcerative colitis. *J Pharmacol Sci* 2004; **96**:307–13.

9 Weigmann B, Lehr HA, Yancopoulos G et al. The transcription factor NFATc2 controls IL-6-dependent T cell activation in experimental colitis. *J Exp Med* 2008; **205**:2099–110.

10 Boirivant M, Fuss IJ, Chu A, Strober W. Oxazolone colitis: a murine model of T helper cell type 2 colitis treatable with antibodies to interleukin 4. *J Exp Med* 1998; **188**:1929–39.

11 Wills-Karp M, Finkelman FD. Untangling the complex web of IL-4- and IL-13-mediated signaling pathways. *Sci Signal* 2008; **1**:pe55.

12 Mandal D, Levine AD. Elevated IL-13Rα2 in intestinal epithelial cells from ulcerative colitis or colorectal cancer initiates MAPK pathway. *Inflamm Bowel Dis* 2010; **16**:753–64.

13 Arijs I, Li K, Toedter G et al. Mucosal gene signatures to predict response to infliximab in patients with ulcerative colitis. *Gut* 2009; **58**:1612–9.

14 Rosen MJ, Frey MR, Washington MK et al. STAT6 activation in ulcerative colitis: a new target for prevention of IL-13-induced colon epithelial cell dysfunction. *Inflamm Bowel Dis* 2011; **17**:2224–34.

15 Kasaian MT, Marquette K, Fish S et al. An IL-4/IL-13 dual antagonist reduces lung inflammation, airway hyperresponsiveness, and IgE production in mice. *Am J Respir Cell Mol Biol* 2013; **49**:37–46.

16 Martin RM, Brady JL, Lew AM. The need for IgG2c specific antiserum when isotyping antibodies from C57BL/6 and NOD mice. *J Immunol Methods* 1998; **212**:187–92.

17 Finkelman FD, Katona IM, Urban JF Jr, Snapper CM, Ohara J, Paul WE. Suppression of *in vivo* polyclonal IgE responses by monoclonal antibody to the lymphokine B-cell stimulatory factor 1. *Proc Natl Acad Sci USA* 1986; **83**:9675–8.

18 de Villiers WJ, Varilek GW, de Beer FC, Guo JT, Kindy MS. Increased serum amyloid a levels reflect colitis severity and precede amyloid formation in IL-2 knockout mice. *Cytokine* 2000; **12**:1337–47.

19 Ramakers JD, Verstege MI, Thuijls G, Te Velde AA, Mensink RP, Plat J. The PPARγ agonist rosiglitazone impairs colonic inflammation in mice with experimental colitis. *J Clin Immunol* 2007; **27**:275–83.

20 Heller F, Fromm A, Gitter AH, Mankertz J, Schulzke JD. Epithelial apoptosis is a prominent feature of the epithelial barrier disturbance in intestinal inflammation: effect of pro-inflammatory interleukin-13 on epithelial cell function. *Mucosal Immunol* 2008; **1**(Suppl. 1):S58–61.

21 Weber CR, Raleigh DR, Su L, Shen L, Sullivan EA, Wang Y, Turner JR. Epithelial myosin light chain kinase activation induces mucosal interleukin-13 expression to alter tight junction ion selectivity. *J Biol Chem* 2010; **285**:12037–46.

22 Prasad S, Mingrino R, Kaukinen K, Hayes KL, Powell RM, MacDonald TT, Collins JE. Inflammatory processes have differential effects on claudins 2, 3 and 4 in colonic epithelial cells. *Lab Invest* 2005; **85**:1139–62.

23 McDermott JR, Humphreys NE, Forman SP, Donaldson DD, Grencis RK. Intraepithelial NK cell-derived IL-13 induces intestinal pathology associated with nematode infection. *J Immunol* 2005; **175**:3207–13.

24 Knight PA, Brown JK, Pemberton AD. Innate immune response mechanisms in the intestinal epithelium: potential roles for mast cells and goblet cells in the expulsion of adult *Trichinella spiralis*. *Parasitology* 2008; **135**:655–70.

25 Herbert DR, Yang JQ, Hogan SP et al. Intestinal epithelial cell secretion of RELM-β protects against gastrointestinal worm infection. *J Exp Med* 2009; **206**:2947–57.

26 Takahashi K, Imaeda H, Fujimoto T, Ban H, Bamba S, Tsujikawa T, Andoh A. Regulation of eotaxin-3/CC chemokine ligand 26 expression by T helper type 2 cytokines in human colonic myofibroblasts. *Clin Exp Immunol* 2013; **173**:323–31.

27 Morimoto M, Morimoto M, Zhao A et al. Functional importance of regional differences in localized gene expression of receptors for IL-13 in murine gut. *J Immunol* 2006; **176**:491–5.

28 Akiho H, Deng Y, Blennerhassett P, Kanbayashi H, Collins SM. Mechanisms underlying the maintenance of muscle hypercontractility in a model of postinfective gut dysfunction. *Gastroenterology* 2005; **129**:131–41.

29 Barron L, Wynn TA. Fibrosis is regulated by Th2 and Th17 responses and by dynamic interactions between fibroblasts and macrophages. *Am J Physiol Gastrointest Liver Physiol* 2011; **300**:G723–8.

30 Scharl M, Frei S, Pesch T et al. Interleukin-13 and transforming growth factor β synergise in the pathogenesis of human intestinal fistulae. *Gut* 2012; **62**:63–72.

31 Jovani M, Fiorino G, Danese S. Anti-IL-13 in inflammatory bowel disease: from the bench to the bedside. *Curr Drug Targets* 2013; **14**:1444–52.

32 Hoving JC, Kirstein F, Nieuwenhuizen NE, Fick LC, Hobeika E, Reth M, Brombacher F. B cells that produce immunoglobulin E mediate colitis in BALB/c mice. *Gastroenterology* 2012; **142**:96–108.

33 Daniel C, Sartory NA, Zahn N, Schmidt R, Geisslinger G, Radeke HH, Stein JM. FTY720 ameliorates oxazolone colitis in mice by directly affecting T helper type 2 functions. *Mol Immunol* 2007; **44**:3305–16.

34 Sun X, Somada S, Shibata K et al. A critical role of CD30 ligand/CD30 in controlling inflammatory bowel diseases in mice. *Gastroenterology* 2008; **134**:447–58.

35 Engel MA, Khalil M, Siklosi N, Mueller-Tribbensee SM, Neuhuber WL, Neurath MF, Becker C, Reeh PW. Opposite effects of substance P and calcitonin gene-related peptide in oxazolone colitis. *Dig Liver Dis* 2012; **44**:24–9.

36 Camelo A, Barlow JL, Drynan LF et al. Blocking IL-25 signalling protects against gut inflammation in a type-2 model of colitis by suppressing nuocyte and NKT derived IL-13. *J Gastroenterol* 2012; **47**:1198–211.

37 Olszak T, An D, Zeissig S et al. Microbial exposure during early life has persistent effects on natural killer T cell function. *Science* 2012; **336**:489–93.

38 Pushparaj PN, Li D, Komai-Koma M, Guabiraba R, Alexander J, McSharry C, Xu D. Interleukin-33 exacerbates acute colitis via Interleukin-4 in mice. *Immunology* 2013; **140**:70–7.

39 Rosen MJ, Chaturvedi R, Washington MK et al. STAT6 deficiency ameliorates severity of oxazolone colitis by decreasing expression of claudin-2 and Th2-inducing cytokines. *J Immunol* 2013; **190**:1849–58.

40 Vermeire S, Van Assche G, Rutgeerts P. The role of C-reactive protein as an inflammatory marker in gastrointestinal diseases. *Nat Clin Pract Gastroenterol Hepatol* 2005; **2**:580–6.

41 Vermeire S, Van Assche G, Rutgeerts P. Laboratory markers in IBD: useful, magic, or unnecessary toys? *Gut* 2006; **55**:426–31.

42 Banks C, Bateman A, Payne R, Johnson P, Sheron N. Chemokine expression in IBD. Mucosal chemokine expression is unselectively increased in both ulcerative colitis and Crohn's disease. *J Pathol* 2003; **199**:28–35.

43 Egesten A, Eliasson M, Olin AI, Erjefalt JS, Bjartell A, Sangfelt P, Carlson M. The pro-inflammatory CXC-chemokines GRO-α/CXCL1 and MIG/CXCL9 are concomitantly expressed in ulcerative colitis and decrease during treatment with topical corticosteroids. *Int J Colorectal Dis* 2007; **22**:1421–7.

44 Zahn A, Giese T, Karner M, Braun A, Hinz U, Stremmel W, Ehehalt R. Transcript levels of different cytokines and chemokines correlate with clinical and endoscopic activity in ulcerative colitis. *BMC Gastroenterol* 2009; **9**:13.

45 Ashwood P, Harvey R, Verjee T, Wolstencroft R, Thompson RP, Powell JJ. Functional interactions between mucosal IL-1, IL-ra and TGF-β1 in ulcerative colitis. *Inflamm Res* 2004; **53**:53–9.

46 Noble CL, Abbas AR, Cornelius J et al. Regional variation in gene expression in the healthy colon is dysregulated in ulcerative colitis. *Gut* 2008; **57**:1398–405.

47 Kabakchiev B, Turner D, Hyams J et al. Gene expression changes associated with resistance to intravenous corticosteroid therapy in children with severe ulcerative colitis. *PLoS One* 2010; **5**: piie13085.

48 Manolakis AC, Kapsoritakis AN, Tiaka EK, Potamianos SP. Calprotectin, calgranulin C, and other members of the S100 protein family in inflammatory bowel disease. *Dig Dis Sci* 2011; **56**:1601–11.

49 Lawrance IC, Fiocchi C, Chakravarti S. Ulcerative colitis and Crohn's disease: distinctive gene expression profiles and novel susceptibility candidate genes. *Hum Mol Genet* 2001; **10**:445–56.

50 Hanania NA, Noonan MJ, Corren J et al. Efficacy and safety of lebrikizumab in severe uncontrolled asthma: results from the lute and verse phase II randomized, double-blind, placebo-controlled trials. *J Allergy Clin Immunol* 2014; **133**(Suppl. 2):AB402.

51 Reinisch W, Panes J, Page K et al. P516 discrepancy between fecal biomarkers and their intestinal gene expression in ulcerative colitis: results from an anti-IL-13 antibody study. *J Crohns Colitis* 2014; **8**(Suppl. 1):S283.

52 Danese S, Rudzinski J, Brandt W et al. OP011 Tralokinumab (CAT-354), an interleukin 13 antibody, in moderate to severe ulcerative colitis: a phase 2 randomized placebo-controlled study. *J Crohns Colitis* 2014; **8**(Suppl. 1):S7.